

Towards a revised virtual crack closure technique

Paolo S. Valvo

Department of Civil Engineering (Structures), University of Pisa, Italy
E-mail: p.valvo@ing.unipi.it

Keywords: Mixed-mode fracture, energy release rate, virtual crack closure technique.

SUMMARY. The virtual crack closure technique (VCCT) is a well-established method for computing the energy release rate (ERR) when analysing fracture problems via the finite element method. For mixed-mode fracture problems, the VCCT is also commonly used to partition the fracture modes, i.e. to determine the ERR contributions related to fracture modes I, II, and III. A perhaps little known fact, however, is that in some circumstances the standard VCCT predicts physically inconsistent, negative values for the modal contributions to the ERR. Focusing on I/II mixed-mode problems, this paper presents a revised VCCT which furnishes a physically consistent partitioning of fracture modes by associating the mode I and II ERR contributions to the works done in a suitably defined two-step process of closure of the virtually extended crack.

1 INTRODUCTION

The virtual crack closure technique (VCCT) is a well-established method for calculating the energy release rate (ERR) when analysing fracture problems via the finite element method (FEM). The technique is based on the numerical implementation of Irwin's crack closure integral [1], as first proposed for two-dimensional problems by Rybicki and Kanninen [2], and later extended to three-dimensional problems by Shivakumar *et al.* [3]. In recent years, the VCCT has gained great popularity for the study of mixed-mode fracture problems, such as the delamination of composite materials and interfacial fracture between dissimilar materials. In these cases, the VCCT is used to compute not only the total ERR, but also the contributions of the three fracture modes (I or opening, II or sliding, and III or tearing) [4].

A perhaps little known fact, however, is that in some circumstances (for instance, bodies with asymmetric cracks subjected to certain load conditions), the standard VCCT predicts physically inconsistent, negative values for the modal contributions to the ERR. Although this potential shortcoming of the technique has already been mentioned in the literature [5], it does not seem to have received the attention it deserves.

Focusing on I/II mixed-mode fracture problems, we develop a revised VCCT that associates the mode I and II ERR contributions to the works done in a suitably defined two-step process of closure of the virtually extended crack. Furthermore, we suggest an implementation procedure based on computation of flexibility coefficients.

The effectiveness of the proposed method is then tested by considering the problem of a delaminated cantilever beam subjected to bending couples. The overall thickness of the beam is kept constant, while several positions of the delamination are considered to highlight the effects of crack asymmetry. The mode I and II contributions to the ERR are computed using both the standard and revised VCCT. For the sake of comparison, the same quantities are also computed using the analytical solution by Suo and Hutchinson [6]. Thus, the revised VCCT demonstrates its ability to furnish physically consistent predictions also in cases where the standard technique fails.

At a deeper investigation, the physically inconsistent predictions of the standard VCCT could be shown to be due to the lack of energetic orthogonality between the crack-tip force components used to compute the mode I and II ERR contributions. However, a more detailed discussion on this topic – as well as on the phenomena of contact, interpenetration, and friction between the crack surfaces – is postponed to the full version of the present paper [7].

2 STANDARD VCCT

2.1 Computation of ERR

Let us consider the two-dimensional (plane stress or plane strain) problem of a linearly elastic, continuous body of width B , affected by a straight crack of length a , with prescribed loads and kinematic boundary conditions (Fig. 1a). A global Cartesian reference system, Oxz , is fixed with the x - and z -axes respectively parallel and orthogonal to the crack direction. A FEM model of the problem is defined using a mesh made of 4-node elements (Fig. 1b). Let A_1, B_1, C_1, \dots , and A_2, B_2, C_2, \dots , denote the nodes placed on the crack's lower and upper surfaces, respectively. The facing upper and lower nodes are initially bonded together by suitable internal constraints, which can be progressively released in order to simulate crack growth. The initial position of the crack tip is taken to be at node C_1 (coincident with C_2).

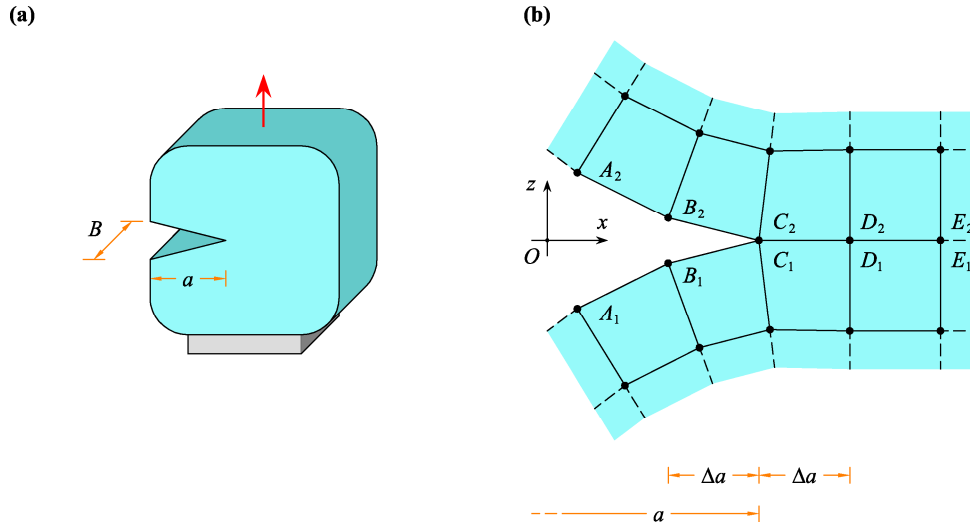


Figure 1: Problem formulation: **a** cracked continuous body; **b** FEM mesh.

According to Irwin [1], the energy dissipated by a virtual (*i.e.* small and kinematically compatible) extension of the crack is equal to the work that would be done to close the crack by the forces that were acting on the new crack surfaces prior to crack extension. Within the FEM framework adopted, the *energy release rate* can then be computed as

$$G = \frac{1}{2B\Delta a} (X_c \Delta u_c + Z_c \Delta w_c), \quad (1)$$

where X_C and Z_C are the internal forces (Fig. 2a) acting at the crack-tip node along the x - and z -directions, respectively, and Δu_C and Δw_C are the corresponding relative displacements (Fig. 2b) that occur when the crack is virtually extended by a length Δa (equal to the size in the x -direction of the elements in the neighbourhood of the crack tip).

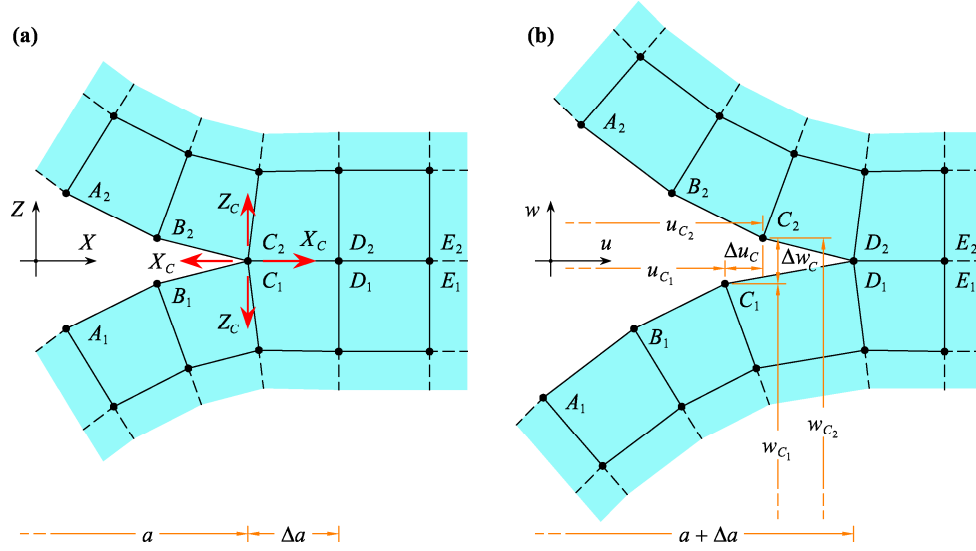


Figure 2: Standard VCCT: **a** crack-tip forces; **b** crack-tip relative displacements.

2.2 Fracture mode partitioning

When crack growth occurs under I/II mixed-mode fracture conditions

$$G = G_I + G_{II}, \quad (2)$$

where G_I and G_{II} are respectively the *mode I and II contributions* to the energy release rate. In line with standard VCCT, the modal contributions are identified simply by the two addends in parentheses in Eq. (1):

$$G_{I,\text{standard}} = \frac{Z_C \Delta w_C}{2B \Delta a} \quad \text{and} \quad G_{II,\text{standard}} = \frac{X_C \Delta u_C}{2B \Delta a}. \quad (3)$$

Now, because of their physical meaning, not only G , but also G_I and G_{II} , must be non-negative quantities [1]. Instead, as the examples in Section 4 below will show, in the case of bodies with asymmetric cracks, Eqs. (3) may yield negative values for some loading conditions. These physically inconsistent results appear when either of the nodal forces, X_C or Z_C , turns out to be opposite in direction with respect to the corresponding relative displacement, Δu_C or Δw_C . To understand why this behaviour occurs, consider that the relative displacements occurring at the crack tip for a virtual crack extension are equal in magnitude (and opposite in sign) to the relative displacements produced by application of the crack-tip forces. Thus, for linear models,

$$\Delta u_C = f_{xx} X_C + f_{xz} Z_C \quad \text{and} \quad \Delta w_C = f_{zx} X_C + f_{zz} Z_C, \quad (4)$$

where f_{xx} , f_{xz} , f_{zx} , and f_{zz} are *flexibility coefficients* ($f_{xz} = f_{zx}$ by virtue of Betti–Maxwell’s reciprocity theorem).

From Eqs. (4) it can be seen that, if $f_{xz} \neq 0$ (which is generally true for bodies with asymmetric cracks), there is a coupling between the crack-tip force in the z -direction and the relative displacement in the x -direction and, *vice versa*, between the crack-tip force in the x -direction and the relative displacement in the z -direction. As will be shown in the following, this coupling has to be taken into account carefully in order to obtain physically consistent partitioning of the fracture modes.

By substituting Eqs. (4) into (1), we obtain the ERR as a quadratic form of the crack-tip forces,

$$G = \frac{1}{2B \Delta a} (f_{xx} X_C^2 + 2f_{xz} X_C Z_C + f_{zz} Z_C^2). \quad (5)$$

A physically consistent method for fracture mode partitioning requires decomposing G into the sum of two non-negative contributions related to fracture modes I and II. Inspection of Eq. (5) leads quite naturally to the assumption that the (non-negative) terms depending on f_{xx} and f_{zz} are related to G_{II} and G_I , respectively. Instead, how to partition the term (undefined in sign) depending on the coupling flexibility coefficient, f_{xz} , is not so obvious. By substituting Eqs. (4) into (3), we obtain

$$G_{I,\text{standard}} = \frac{1}{2B \Delta a} (f_{zz} Z_C^2 + f_{xz} X_C Z_C) \quad \text{and} \quad G_{II,\text{standard}} = \frac{1}{2B \Delta a} (f_{xx} X_C^2 + f_{xz} X_C Z_C), \quad (6)$$

hence, according to the standard VCCT, the term depending on f_{xz} is equally partitioned between G_I and G_{II} . Since the abovementioned term is undefined in sign, it is predictable that in some circumstances negative values for G_I and G_{II} can be obtained using the standard VCCT.

3 REVISED VCCT

3.1 Physically consistent partitioning of fracture modes

The revised VCCT proposed here takes the contributions G_I and G_{II} as associated to the works done in a suitably defined two-step closure process of the virtually extended crack. In step I, corresponding to fracture mode I (opening), the crack-tip relative displacement in the z -direction, Δw_C , is closed completely by applying the necessary crack-tip force, $Z_C^{(I)}$, in the same z -direction. At the same time, a null force, $X_C^{(I)} = 0$, is applied in the x -direction, but, because of coupling, the crack-tip relative displacement in the x -direction, Δu_C , is partly closed (if $f_{xz} > 0$), or further opened (if $f_{xz} < 0$), by a quantity $\Delta u_C^{(I)}$ (Fig. 3a). In step II, corresponding to fracture mode II (sliding), the residual crack-tip relative displacement in the x -direction, $\Delta u_C^{(II)} = \Delta u_C - \Delta u_C^{(I)}$, is closed by applying suitable crack-tip forces, $X_C^{(II)} = X_C$ and $Z_C^{(II)} = Z_C - Z_C^{(I)}$ (Fig. 3b).

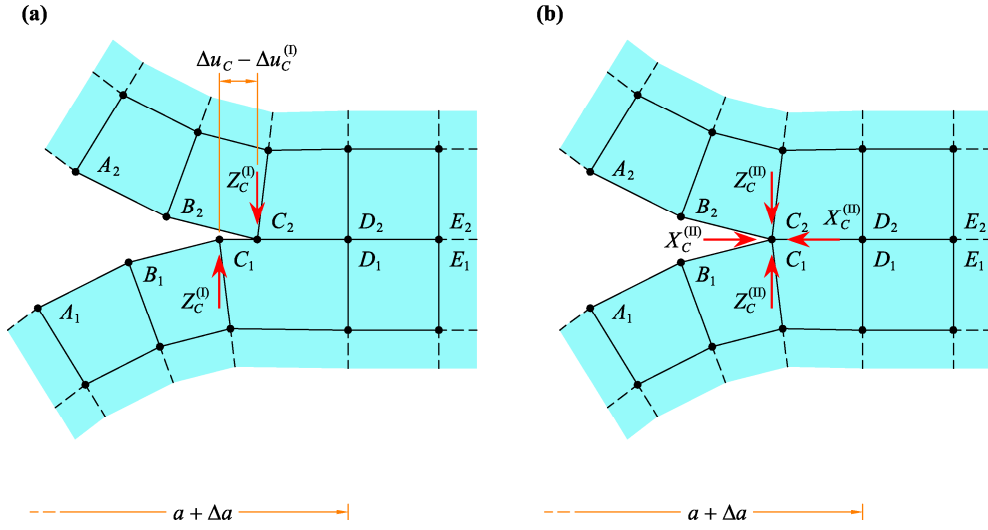


Figure 3: Revised VCCT: **a** step I, closure of the crack-tip relative displacement in the z -direction (mode I); **b** step II, closure of the crack-tip relative displacement in the x -direction (mode II).

By using Eqs. (4), the crack-tip forces to be applied in step I are determined as

$$X_C^{(0)} = 0 \quad \text{and} \quad Z_C^{(0)} = \frac{\Delta w_C}{f_{zz}} = \frac{f_{xz}}{f_{zz}} X_C + Z_C. \quad (7)$$

These forces produce the crack-tip relative displacements

$$\Delta u_C^{(0)} = f_{xz} Z_C^{(0)} = \frac{f_{xz}}{f_{zz}} \Delta w_C \quad \text{and} \quad \Delta w_C^{(0)} = f_{zz} Z_C^{(0)} = \Delta w_C. \quad (8)$$

Note that by virtue of Eqs. (7), in the presence of coupling ($f_{xz} \neq 0$), $Z_C^{(0)}$ is generally different from the actual crack-tip force, Z_C .

The crack-tip forces to be applied in step II are the total crack-tip force in the x -direction and the residual crack-tip force in the z -direction,

$$X_C^{(II)} = X_C \quad \text{and} \quad Z_C^{(II)} = Z_C - Z_C^{(0)} = -\frac{f_{xz}}{f_{zz}} X_C. \quad (9)$$

By using Eqs. (4), (7), (8), and (9), the ensuing crack-tip relative displacements are determined as

$$\Delta u_C^{(II)} = \left(f_{xx} - \frac{f_{xz}^2}{f_{zz}}\right) X_C = \Delta u_C - \Delta u_C^{(0)} \quad \text{and} \quad \Delta w_C^{(II)} = 0. \quad (10)$$

Therefore, in step II the residual crack-tip relative displacement in the x -direction is cancelled exactly, while no further relative displacement in the z -direction is produced.

Accordingly, the mode I and II contributions to the ERR are

$$G_I = \frac{Z_C^{(I)} \Delta w_C^{(I)}}{2B \Delta a} \quad \text{and} \quad G_{II} = \frac{X_C^{(II)} \Delta u_C^{(II)}}{2B \Delta a}. \quad (11)$$

By substituting Eqs. (7)–(10) into (11), we obtain

$$G_I = \frac{1}{2B \Delta a} \frac{\Delta w_C^2}{f_{zz}} \quad \text{and} \quad G_{II} = \frac{f_{xx} f_{zz} - f_{xz}^2}{2B \Delta a} \frac{X_C^2}{f_{zz}}, \quad (12)$$

which are clearly non-negative quantities. Thus, in contrast to the standard VCCT, the revised VCCT furnishes a physically consistent partitioning of the fracture modes. Eqs. (12) also reveal the conditions for pure fracture modes: pure mode I ($G_{II} = 0$) is obtained for $X_C = 0$, pure mode II ($G_I = 0$) for $\Delta w_C = 0$.

3.2 Implementation procedure

In standard FEM analysis, nodal displacements are used as the principal unknowns, while nodal forces are computed from element stresses as secondary results. Therefore, it would be preferable to determine G_I and G_{II} based on the values of the crack-tip relative displacements alone. To this aim, we substitute Eqs. (4) into the second of Eqs. (12) to obtain

$$G_I = \frac{1}{2B \Delta a} \frac{\Delta w_C^2}{f_{zz}} \quad \text{and} \quad G_{II} = \frac{1}{2B \Delta a} \frac{1}{f_{zz}} \frac{(f_{zz} \Delta u_C - f_{xz} \Delta w_C)^2}{f_{xx} f_{zz} - f_{xz}^2}. \quad (13)$$

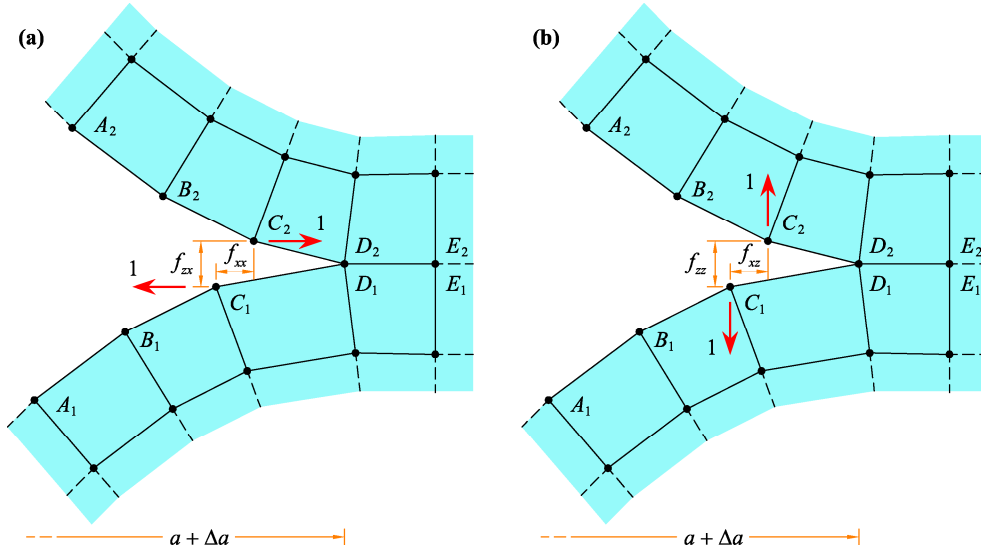


Figure 4: Computation of flexibility coefficients: **a** unit forces in the x -direction; **b** unit forces in the z -direction.

The flexibility coefficients entering into Eqs. (13) can be readily evaluated by considering the FEM mesh with the virtually extended crack and conducting two preliminary analyses for when unit forces are applied at nodes C_1 and C_2 in the x - and z -directions, respectively (Fig. 4a and 4b). The flexibility coefficients are equal to the corresponding relative displacements:

$$\begin{aligned} f_{xx} &= (u_{C_2} - u_{C_1})|_{x_c=1}, & f_{zx} &= (w_{C_2} - w_{C_1})|_{x_c=1}; \\ f_{xz} &= (u_{C_2} - u_{C_1})|_{z_c=1}, & f_{zz} &= (w_{C_2} - w_{C_1})|_{z_c=1}. \end{aligned} \quad (14)$$

4 APPLICATIVE EXAMPLE

4.1 Test problem

The effectiveness of proposed method is now tested by considering the problem shown in Figure 5, where a delaminated cantilever beam is subjected to two bending couples, M_1 and M_2 .

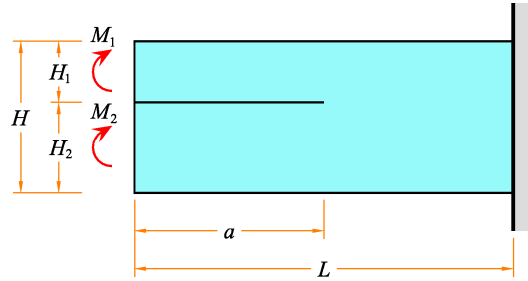


Figure 5: Delaminated cantilever beam subjected to bending couples.

The beam is of length $L = 100$ mm, width $B = 25$ mm, and thickness $H = 10$ mm. The crack length is $a = 50$ mm. The delamination splits the beam into two sublaminae of thicknesses H_1 and H_2 . Several values of the *thickness ratio*, $\eta = H_1 / H_2$, are considered in order to highlight the effects of crack asymmetry. The material is homogeneous, isotropic, and linearly elastic. The Young modulus and Poisson ratio are respectively $E = 100$ GPa and $\nu = 0.3$. A FEM model of the delaminated beam has been developed using ABAQUS® software with CPS8 (8-node quadratic plane stress) elements (Fig. 6). The element size in the crack-tip region is $\Delta a = 0.5$ mm.

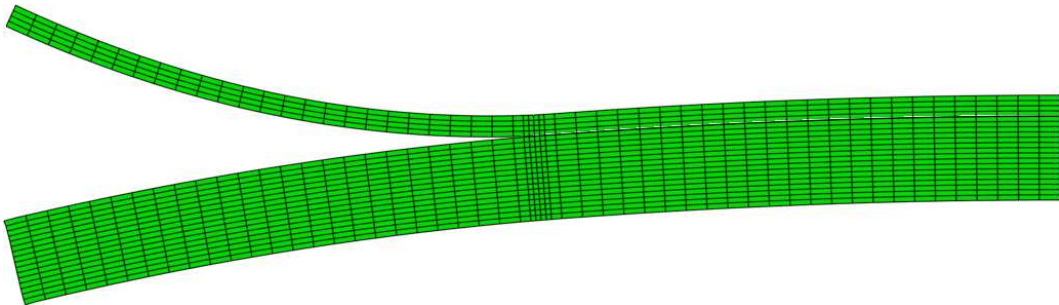


Figure 6: FEM model of the delaminated cantilever beam ($\eta = 4/16$, $M_1 = 1$ N m, $M_2 = -20$ N m).

4.2 Analysis results

Figure 7 shows the mode I and II contributions to the ERR for fixed $M_1 = 1 \text{ N m}$ and variable M_2 , for four select values of the thickness ratio, η . Triangles and circles denote values computed using the standard and revised VCCT through Eqs. (3) and (13), respectively. Continuous lines, reported for reference, represent the analytical solution by Suo and Hutchinson [6].

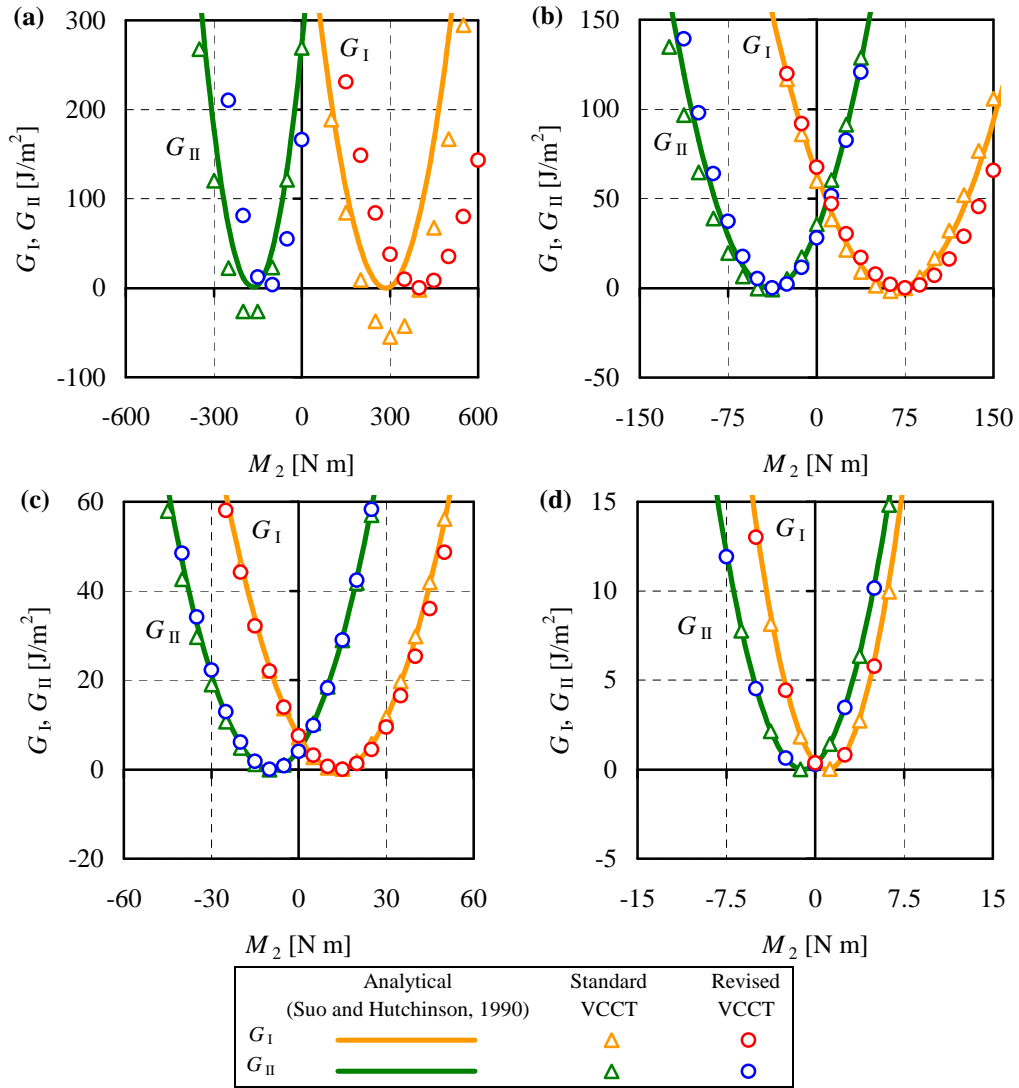


Figure 7: Mode I and II ERR contributions as functions of the bending moment in the lower sublaminate: **a** $\eta = 1/19$; **b** $\eta = 2/18$; **c** $\eta = 4/16$; **d** $\eta = 10/10 = 1$.

For the maximum crack asymmetry considered (Fig. 7a), both the standard and revised VCCT differ to varying degrees from the analytical solution. Most notably, the standard VCCT yields

physically inconsistent, negative values for G_I and G_{II} in certain ranges of M_2 . As the asymmetry decreases (Figs. 7b and 7c), the discrepancies between the analytical and numerical predictions diminish as well. Lastly, in the case of a symmetric crack (Fig. 7d), the predictions of the standard and revised VCCT coincide exactly and both agree very well with the analytical solution.

Physical inconsistencies in the standard VCCT can moreover be highlighted by examining the plot of the *relative modal contributions to G*,

$$\gamma_I = \frac{G_I}{G} \quad \text{and} \quad \gamma_{II} = \frac{G_{II}}{G}, \quad (15)$$

as functions of the bending moment in the lower sublaminate, M_2 (Fig. 8). Negative values of G_I correspond to $\gamma_I < 0$ and $\gamma_{II} > 1$; likewise, negative values of G_{II} correspond to $\gamma_I > 1$ and $\gamma_{II} < 0$. However, values of γ_I and γ_{II} greater than unity are not physically acceptable, as they would imply that one of the two modal contributions to G is greater than the whole.

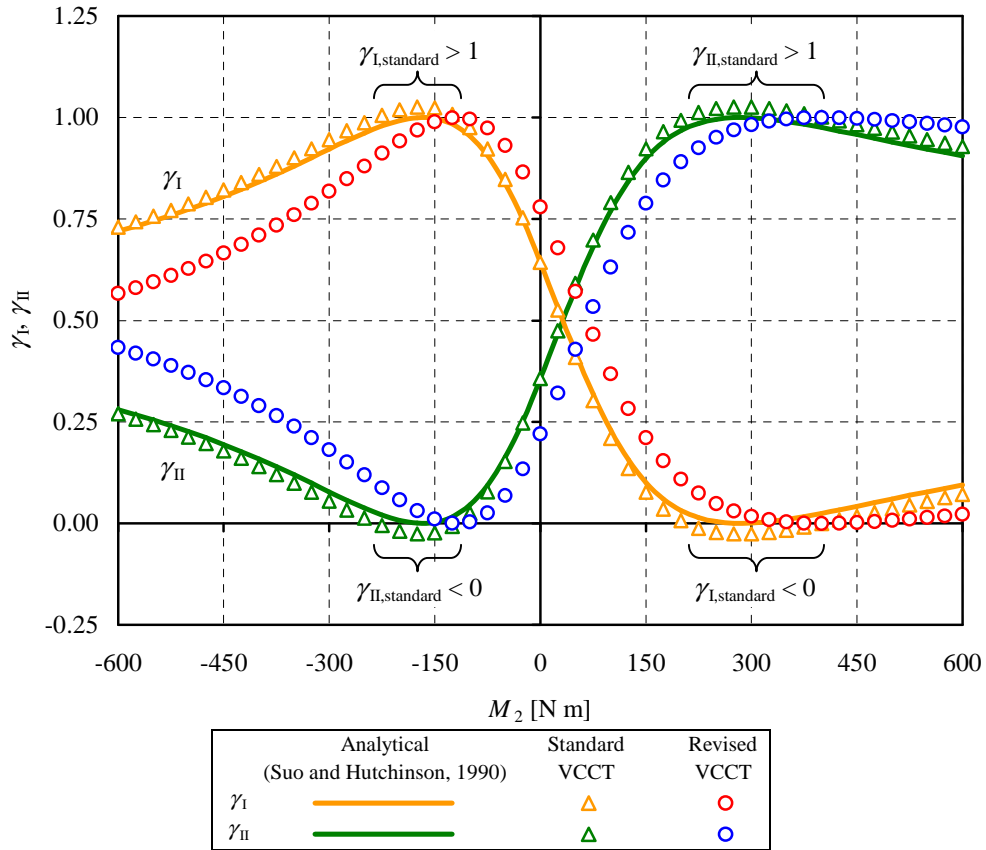


Figure 8: Relative modal contributions to the ERR as functions of the bending moment in the lower sublaminate ($\eta = 1/19$).

5 CONCLUSIONS

The study has brought to light a weak point in the standard VCCT, which in some circumstances predicts physically inconsistent, negative values for the modal contributions to the ERR. In particular, for I/II mixed-mode fracture problems, this behaviour can be observed in the case of bodies with asymmetric cracks for which there is a coupling (indicated by $f_{xz} \neq 0$) between the crack-tip forces and relative displacements in the x - and z -directions (respectively, parallel and orthogonal to the crack direction).

To overcome this drawback, a revised VCCT has been developed, which associates the mode I and II ERR contributions to the works done in a suitably defined two-step process of closure of the virtually extended crack. An implementation procedure has also been suggested based on computation of flexibility coefficients, which can be incorporated simply and effectively into any existing FEM package.

The effectiveness of the proposed method has been tested by considering the problem of a delaminated cantilever beam subjected to bending couples. The overall thickness of the beam is kept constant, while several positions of the delamination are considered to highlight the effects of crack asymmetry. The mode I and II contributions to the ERR, G_I and G_{II} , have been computed using the standard and revised VCCT, as well as the analytical solution by Suo and Hutchinson [6]. While no significant differences can be observed between the predictions for the total G via the compared methods, the predictions for G_I and G_{II} coincide only for the case of a symmetrical crack, and diverge increasingly as crack asymmetry grows. For the largest crack asymmetry considered (thickness ratio $\eta = 1/19$), manifestly inconsistent, negative values for G_I and G_{II} are obtained using the standard VCCT, while the revised VCCT has consistently proven able to furnish a physically consistent partitioning of the fracture modes.

At a deeper investigation, the physically inconsistent predictions of the standard VCCT could be shown to be due to the lack of energetic orthogonality between the crack-tip force components used to compute the modal contributions to the ERR. Energetic orthogonality is instead ensured between the crack-tip force components considered by the revised VCCT. However, a more detailed discussion on this topic – as well as on the phenomena of contact, interpenetration, and friction between the crack surfaces – is postponed to the full version of the present paper [7].

References

- [1] Irwin, G.R., “Fracture”, in *Handbuch der Physik*, Flugge, S. (ed.), vol. VI, Springer, Berlin, 551–590 (1958).
- [2] Rybicki, E.F., Kanninen, M.F., “A finite element calculation of stress intensity factors by a modified crack closure integral”, *Engng. Fract. Mech.*, **9**, 931–938 (1977).
- [3] Shivakumar, K.N., Tan, P.W., Newman, J.C., “A virtual crack-closure technique for calculating stress intensity factors for cracked three dimensional bodies”, *Int. J. Fract.*, **36**, R43–R50 (1988).
- [4] Krueger, R., “Virtual crack closure technique: History, approach, and applications”, *Appl. Mech. Rev.*, **57**, 109–143 (2004).
- [5] Wang, S., Guan, L., “On fracture mode partition theories”, *Comput. Mater. Sci.* (in press).
- [6] Suo, Z., Hutchinson, J.W., “Interface crack between two elastic layers”, *Int. J. Fract.*, **43**, 1–18 (1990).
- [7] Valvo, P.S., “A revised virtual crack closure technique for physically consistent fracture mode partitioning”, *Int. J. Fract.* (submitted).